AFRL-RX-WP-TP-2009-4091

PROBABILISTIC SENSITIVITY ANALYSIS OF FRETTING FATIGUE (Preprint)

Patrick J. Golden, Harry R. Millwater, and Xiaobin Yang

Behavior/Life Prediction Section
Metals Branch

APRIL 2009
Interim Report

AIR FORCE RESEARCH LABORATORY
MATERIALS AND MANUFACTURING DIRECTORATE
WRIGHT-PATTERSON AIR FORCE BASE, OH 45433-7750
AIR FORCE MATERIEL COMMAND
UNITED STATES AIR FORCE

REPORT DOCUMENTATION PAGE

Form Approved
OMB No. 0704-0188

1. REPORT DATE *(DD-MM-YY)*	2. REPORT TYPE	3. DATES COVERED *(From - To)*
April 2009	Journal Article Preprint	01 April 2009 – 01 April 2009

4. TITLE AND SUBTITLE
PROBABILISTIC SENSITIVITY ANALYSIS OF FRETTING FATIGUE (Preprint)

5a. CONTRACT NUMBER
FA8650-06-C-5060

5b. GRANT NUMBER

5c. PROGRAM ELEMENT NUMBER
62102F

6. AUTHOR(S)
Patrick J. Golden (Metals Branch, Behavior/Life Prediction Section (AFRL/RXLMN))
Harry R. Millwater and Xiaobin Yang (University of Texas at San Antonio)

5d. PROJECT NUMBER
4347

5e. TASK NUMBER
RG

5f. WORK UNIT NUMBER
M02R3000

7. PERFORMING ORGANIZATION NAME(S) AND ADDRESS(ES)

Metals Branch, Behavior/Life Prediction Section (AFRL/RXLMN)
Materials and Manufacturing Directorate
Air Force Research Laboratory
Wright-Patterson Air Force Base, OH 45433-7750
Air Force Materiel Command, United States Air Force

University of Texas at San Antonio

8. PERFORMING ORGANIZATION REPORT NUMBER
AFRL-RX-WP-TR-2009-4091

9. SPONSORING/MONITORING AGENCY NAME(S) AND ADDRESS(ES)

Air Force Research Laboratory
Materials and Manufacturing Directorate
Wright-Patterson Air Force Base, OH 45433-7750
Air Force Materiel Command
United States Air Force

10. SPONSORING/MONITORING AGENCY ACRONYM(S)
AFRL/RXLMN

11. SPONSORING/MONITORING AGENCY REPORT NUMBER(S)
AFRL-RX-WP-TR-2009-4091

12. DISTRIBUTION/AVAILABILITY STATEMENT
Approved for public release; distribution unlimited.

13. SUPPLEMENTARY NOTES
PAO case number WPAFB 09-1276; date cleared: 01 April 2009. The U.S. Government is joint author of this work and has the right to use, modify, reproduce, release, perform, display, or disclose the work. Submitted to AIAA Structure, Structural Dynamics and Materials Conference, Palm Springs, CA. Document contains color.

14. ABSTRACT
A probabilistic analysis of the fatigue life of specimens subject to fretting fatigue was carried out. A mechanics based fretting life analysis was applied that accounted for the local stress gradient at the edge of contact. The random variables in the analysis included the initial crack size, coefficient of friction, crack growth rate law, and the contact pad profile. The variation in pad profiles was determined through statistical analysis of seventy-seven machined pads. A probabilistic fatigue analysis was applied using Monte Carlo sampling to determine the statistics (mean and standard deviation) of the fatigue life prediction and the probabilistic sensitivities (partial derivatives of the fatigue statistics with respect to the input probability density function parameters).

15. SUBJECT TERMS
probabilistic analysis, fretting fatigue, crack size

16. SECURITY CLASSIFICATION OF:			17. LIMITATION OF ABSTRACT:	18. NUMBER OF PAGES	19a. NAME OF RESPONSIBLE PERSON (Monitor)
a. REPORT	b. ABSTRACT	c. THIS PAGE			Reji John
Unclassified	Unclassified	Unclassified	SAR	18	19b. TELEPHONE NUMBER *(Include Area Code)* (937) 255-9791

Standard Form 298 (Rev. 8-98)
Prescribed by ANSI Std. Z39-18

Probabilistic Sensitivity Analysis of Fretting Fatigue

Patrick J. Golden*
Air Force Research Laboratory, Wright-Patterson AFB, OH 45433

Harry R. Millwater† and Xiaobin Yang‡
University of Texas at San Antonio, San Antonio, TX 78249

A probabilistic analysis of the fatigue life of specimens subject to fretting fatigue was carried out. A mechanics based fretting life analysis was applied that accounted for the local stress gradient at the edge of contact. The random variables in the analysis included the initial crack size, coefficient of friction, crack growth rate law, and the contact pad profile. The variation in pad profiles was determined through statistical analysis of seventy-seven machined pads. A probabilistic fatigue analysis was applied using Monte Carlo sampling to determine the statistics (mean and standard deviation) of the fatigue life prediction and the probabilistic sensitivities (partial derivatives of the fatigue statistics with respect to the input probability density function parameters).

Nomenclature

α	=	slope of shear force versus normal force in partial slip
μ	=	coefficient of friction
σ_{ij}	=	components of stress
a	=	crack depth
c	=	half surface crack length
F	=	applied load in the fretting test
$h(x)$	=	contact gap function
K	=	stress intensity factor
M	=	contact moment
R	=	load ratio
$p(x)$	=	contact pressure traction
P	=	normal contact force
$q(x)$	=	contact shear traction
Q	=	shear contact force

I. Introduction

Fretting is a problem in many aerospace applications including the blade to disk attachment in turbine engines. Two fretting modes can contribute to damage in fretting: gross slip when the two surfaces slide resulting in wear, and partial slip when the two surfaces are nominally stuck together except for a small slip zone at the edge contact. The surface damage and wear caused by fretting is a costly maintenance burden and when combined with the very high local contact stresses due to fretting, it can result in disk or blade cracking and the potential for catastrophic failure. A probabilistic analysis is often applied to problems to help determine the effect of variability of the model input parameters on the model outputs. Prior work on statistical or probabilistic analysis in fretting includes modeling of the variability in the contact surface profile by Kumari and Farris [1]. Here, the measured profiles of the indentors in fretting fatigue tests were measured and statistically described and carried through the life prediction models to estimate the expected variability in stress and life. Other probabilistic fretting analyses include work on fretting fatigue of riveted lap joints [2] and on rolling contact [3]. The objective of the current work is to develop and demonstrate a probabilistic fretting fatigue lifing approach for a dovetail fretting experimental configuration that

* Materials Research Engineer, Metals, Ceramics & NDE Division, 2230 Tenth St, Ste 1, Senior Member
† Associate Professor, Dept. of Mechanical Engineering, One UTSA Circle, Member
‡ Graduate Student, Dept. of Management Science and Statistics, One UTSA Circle

includes a broad range of input random variables, and to apply efficient sensitivity methods to determine the relative importance of the input variables. A previously demonstrated stress and life prediction analysis is adapted to this effort. Input probability density functions (PDF's) were developed using available laboratory data. A modular probabilistic sensitivity code was developed and applied to this analysis.

II. Deterministic Fretting Analysis

A series of fretting experiments was previously conducted [4] to improve understanding of fretting behavior in Ti-6Al-4V and to test life prediction models. The geometry of the fretting samples was a dovetail shaped specimen that was designed to represent the attachment between a turbine engine blade and disk. The tests were conducted at room temperature, which is consistent with the operating conditions of a fan disk. The contact interface was bare Ti-6Al-4V on bare Ti-6Al-4V, but several coatings and residual stress surface treatments applied to the contact interface were also tested. The analysis in the current work was limited to the bare Ti-6Al-4V tests. A schematic of the fretting fatigue test rig modeled in this analysis is shown in Figure 1. The experimental setup consists of the dovetail specimen (one-half of the specimen is shown in schematic), two fretting pads, and a steel fixture. The fretting pads are held in the steel fixture at a 45° flank angle, and the dovetail specimen is pulled with a cyclic load, F, into the fretting pads. Both the dovetail specimen and pads were machined from Ti-6Al-4V with a thickness of 7.62 mm, modulus E = 116 GPa, and Poisson's ratio ν = 0.31. The nominal fretting pad geometry was a 3 mm flat with 3 mm blending radii. The normal, P, and shear, Q, contact forces were measured indirectly from strain gage instrumentation of the experiments. More details of the experimental setup and instrumentation can be found in Golden and Nicholas [4]. 10 tests were run at values of F_{max} ranging from 18 kN to 30 kN at a load ratio R = 0.1.

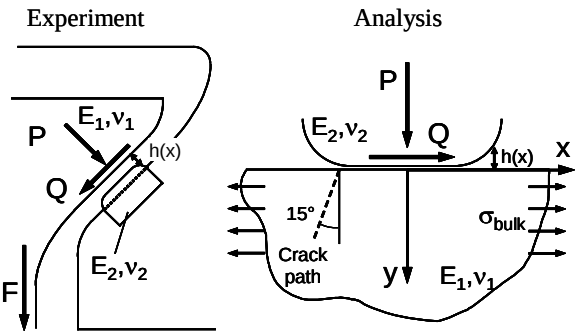

Figure 1. Schematic of the dovetail experiment and the analysis.

A fracture mechanics based fretting life prediction analysis for dovetail specimens was developed and demonstrated using these and other experimental test data and is described in Golden and Calcaterra [5]. The objective of this prior work was to demonstrate lifing methods that could be applied to more complex 3-D structures found in turbine engines, however, the current problem can be simplified to a 2-D problem. The analysis was broken into two parts: a finite element method (FEM) analysis and a 2-D numerical contact stress analysis. A finite element analysis is needed in this problem to determine two sets of quantities. The first quantity, described here, relates to the behavior of the contact force history. The second, which can be obtained from the same FEM model, is the bulk stress as shown in Figure 1 and is described below. The dovetail geometry was modeled using a nonlinear contact FEM model. This analysis yields the contact force history for P and Q and an example is plotted in Figure 2. This example shows a single loading and unloading starting from no load. As the load is applied, the contact is initially in sliding (gross slip) and the contact forces follow the dashed line defined by the equation

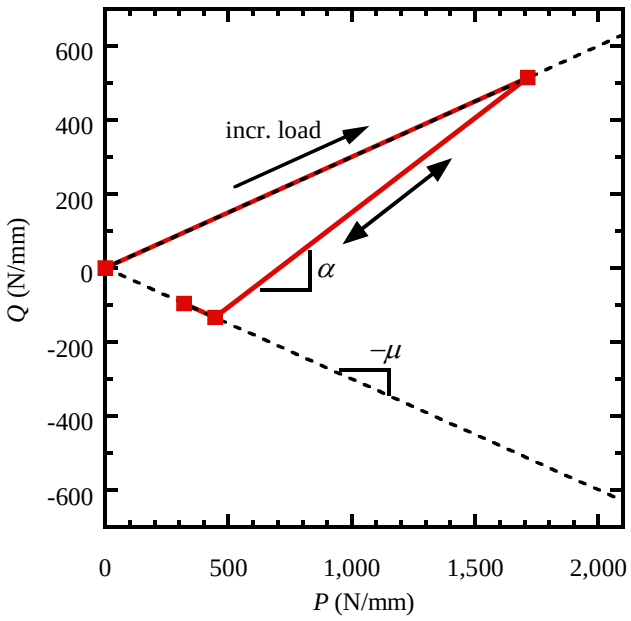

Figure 2. A typical plot of Q versus P showing the partial slip slope α and the boundaries defined by μ

$$Q = \mu P \tag{1}$$

where μ is the coefficient of friction. Upon load reversal, the contact load path changes slope to the partial slip slope, α, which is a characteristic of the component geometry and compliance. The contact forces will follow the slope α for both increasing and decreasing loads until the dashed lines defining friction are reached. Therefore, the two key inputs needed for prediction of the contact force history for a given applied load history are μ and α. The coefficient of friction is a property that can only be measured, however, α can be predicted from the FEM analysis or measured by experiment. Once these 2 parameters are known, the contact forces can be determined for a given applied force without additional FEM analysis through a procedure developed by Gean and Farris [6].

Once the contact forces were known, the contact stresses were calculated using a 2-D numerical contact stress analysis. Figure 1 shows a schematic of the equivalent contact geometry, defined by the gap function, $h(x)$, used in this analysis. In the experiments described here, $h(x)$ was simply the profile of the fretting pads that are pressed into contact with the flat dovetail specimens. Rather than use the prescribed profiles in the analysis, the as-machined profiles were obtained using a contacting profilometer to quantify the actual profiles. The analytical tool, CAPRI (Contact Analysis for Profiles of Random Indenters) described in McVeigh et al. [7], was developed to solve the singular integral equation that defines this contact problem using any reasonable function, $h(x)$, as measured from the profilometry. The output of CAPRI is the pressure, $p(x)$, and shear, $q(x)$, tractions due to the applied contact forces. An example of these tractions is shown in Figure 3. Next, CAPRI was used to determine the subsurface stress field under the contact due to $p(x)$ and $q(x)$. Note the peaks located near the edges of contact in Figure 3. These peaks in the pressure, shear, and the subsurface stresses were driven by the geometry near the edges of contact and typically result in crack initiation and growth from the edge of contact.

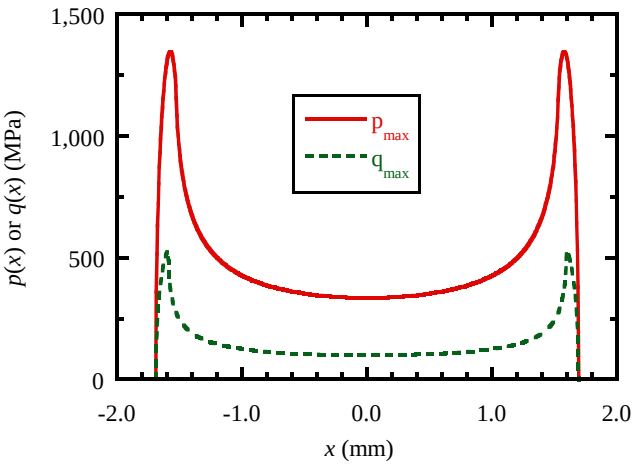

Figure 3. Pressure and shear tractions from CAPRI

The last step in the analysis is the fracture mechanics based fatigue crack growth prediction. Here, the total stresses along the expected crack growth path are needed to calculate the stress intensity factor range, ΔK. To get the total stress solution both the contact stresses from CAPRI and the bulk stress as shown in Figure 1 were superposed. The bulk stress was the stress distribution induced in the component due to the remotely applied loading and the geometry of the component. A procedure to obtain the bulk stress distribution for a dovetail geometry was described by Golden and Calcaterra [5] which required both the FEM model and CAPRI results. Once the full subsurface stress distribution was known, the mode I stress gradient could be extracted along the expected crack path at the edge of contact. Since the stress gradient was nonlinear, weight function stress intensity factor solutions were applied [8]. The crack propagation life was then integrated using a crack growth model of the form

$$\frac{da}{dN} = f(\Delta K) \tag{2}$$

where da/dN is the crack growth rate. Integration of life was performed using the Euler method starting from a small initial fretting crack typically 25 mm in depth, until fracture. Crack growth properties from previous testing on the same Ti-6Al-4V material used in the US Air Force High Cycle Fatigue program [9] were used.

III. Statistical Analysis

The random variables for the probabilistic fretting analysis performed in this study were chosen from the key input variables of the deterministic analysis described above. These key input variables included the initial crack size, the coefficient of friction, the slope α that defines the contact forces during partial slip, the crack growth law parameters, and the parameters defining the shape of the pad profile. PDF's were developed for each of these

random variables from measurements and test data available both from the dovetail fretting experiments and from other fatigue and fatigue crack growth experiments. The details of the development of these PDF's are described below. A summary of the resulting PDF's are shown in Table 1.

A. Initial crack size

The deterministic fretting fatigue life prediction analysis described above is based on fracture mechanics based crack propagation. To perform this analysis an initial crack size is required. Previous work [8] has shown that the initial fretting cracks tend to be shallow, low aspect ratio (a/c) surface cracks that often appear to be several shallow micro-cracks that have coalesced. Here, a is the surface crack depth and c is the half surface length. Investigations of naturally initiated cracks in smooth bar fatigue specimens in Ti-6Al-4V with the same microstructure [10] have revealed that the cracks appear to initiate almost exclusively at primary alpha grains that intersect the surface of the specimen. These naturally initiated cracks in the primary alpha grains form readily identifiable facets on the specimen fracture surface. Measurements of these initial cracks were made in a prior study [10] on fatigue variability of Ti-6Al-4V, where repeated tests were conducted at a few constant amplitude stress levels. The resulting distribution of primary alpha grain facets was used here to represent the expected variability in initial fretting crack depth. Since it has been shown that typically multiple surface cracks form and coalesce in fretting, a constant, low aspect ratio of a/c = 0.2 was used. The mean and standard deviation of the measured naturally initiated crack sizes is listed in Table 1. It was determined that a lognormal distribution was the best fit to the data.

B. Coefficient of friction and the partial slip slope

As described above and depicted in Figure 2, the coefficient of friction and the partial slip slope of Q versus P were measured during each test. The accuracy of these measurements, however, was limited to the accuracy of the strain gage instrumentation of the tests and the finite element analysis that was used to convert fixture strain to applied load. Additionally, variability in friction was expected from test to test. Both the measurement uncertainty and inherent variability in the tests needed to be captured in the probabilistic model. To achieve this, data was collected from twenty-three fretting tests all of which were conducted under similar loading conditions. All tests were bare Ti-6Al-4V on Ti-6Al-4V contact (no coatings) and all were loaded at R = 0.1. The measured values of friction coefficient and partial slip slope, α, were found to be correlated since. The uncertainty in the expected values of friction and partial slip slope along with their correlation was modeled using a multivariate normal distribution. The results are tabulated in Table 1.

C. Fatigue crack growth parameters

The crack growth rate curves used for crack propagation predictions were based on fatigue crack growth tests previously conducted [9]. Four tests from two different labs were fit to a bilinear Paris crack growth model for R = 0.1 and -1, where, da/dN is the crack growth rate and ΔK is the stress intensity factor range. The Walker model [11] was used to collapse the data from the different R values using an equation of the form

$$\begin{aligned} da/dN &= C_1\left[\Delta K(1-R)^{(m-1)}\right]^{n_1} \qquad \Delta K < b \\ da/dN &= C_2\left[\Delta K(1-R)^{(m-1)}\right]^{n_2} \qquad \Delta K \geq b \end{aligned} \tag{3}$$

where b is the intersection point for regions 1 and 2, defined as

$$b = \frac{\log_{10} C_1 - \log_{10} C_2}{n_2 - n_1} \tag{4}$$

The values of the Walker exponent m were determined in the previous program [9] and different values were used for $R < 0$ and $R > 0$. The statistics of the curve fit were modeled using a multivariate normal. The coefficient C_i and the exponent n_i were found to be correlated for each segment of the bilinear crack growth model. The mean, standard deviation, and correlation coefficients are summarized in Table 1. The values of the model parameters resulted units of MPa$\sqrt{}$m for ΔK, and m/cycle for da/dN.

D. Pad profile

The nominal geometry for the contact pad is shown in Figure 4. The prescribed profile is the geometry that was requested on the part drawings provided to the machine shop. The central segment of the prescribed profile is flat with a length of 3.00 mm. The edges of the profile have constant radii of 3.0 mm. Due to variations due to machining, however, the as-machined profiles differ from the prescribed profile in the part drawing. The contact pad profiles were measured using a contacting profilometer prior to being tested. The contact profilometer had a vertical resolution of approximately 10 nm. Two examples of measured profiles are plotted in Figure 2. Note that the scale on the y-axis is significantly magnified to highlight variations in the measured profiles. It is clear from these measured profiles that the central flat section of the pad is not truly flat and that the radii at the edges do not always match the prescribed radii either in position or sharpness. Additionally, there is measurable variability in the profile geometry from pad to pad. It was desired to capture this variability through a statistical analysis so it could be used in the subsequent probabilistic analysis. To achieve that objective, seventy-seven contact pads were measured using the contact profilometer.

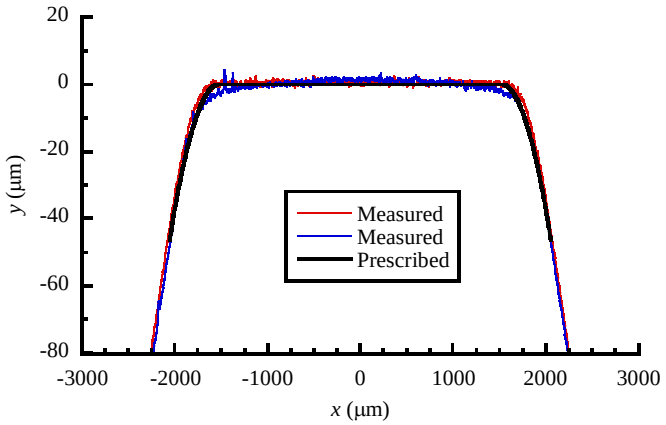

Figure 4. Prescribed and measured machined pad profiles.

In order to model the contact profile variability in the probabilistic analysis, a mathematical description of the contact profile was needed that could capture the important features of the profile. Key features were believed to be the actual radii of the edges of the pad as these can significantly affect the stress at the edge of contact. Also important was the flatness of the central portion of the pad. A rounded pad versus a very flat pad could also significantly affect the contact stresses. A piecewise curve with twenty-one parameters was defined to represent the measured contact profiles and was written as

$$y=\begin{cases} k^L x+b^L & x<a_1 \\ y_0^L+\sqrt{\left(R^L\right)^2-\left(x-x_0^L\right)^2} & a_1<x<a_2 \\ c_0+c_1x+c_2x^2+c_3x^3+c_4x^4+c_5x^5+c_6x^6 & a_2<x<a_3 \\ y_0^R+\sqrt{\left(R^R\right)^2-\left(x-x_0^R\right)^2} & a_3<x<a_4 \\ k^R x+b^R & x>a_4 \end{cases} \tag{5}$$

where x and y represent a Cartesian coordinate system with x along the profile and y the height of the profile. The central segment of the profile ($a_2<x<a_3$) was represented by a sixth order polynomial to allow the nominally flat section to have curvature. Just outside the central section were two circular arcs to represent the radii at the edges of contact. Just beyond the radii were flat taper sections. Through various constraints the number of parameters was reduced from twenty-one to thirteen. The constants k^L, k^R, b^L, b^R, y_0^L, x_0^L, x_0^R, R^L, R^R, c_1, c_2, c_3, c_4, c_5, and c_6 were determined from nonlinear regression of each of the measured seventy-seven profiles. These constants were referred to as γ_i, where i ranged from 0 to 12. The remaining 8 constants in Equation 1 were functions of γ_i as defined by the constraints. Scatter plots of these 13 regression parameters are shown in Figure 5, which shows that many of the parameters are highly correlated. Finally, the results of the nonlinear regression from all 77 profiles were fit to a multivariate normal distribution. The mean and standard deviation of the regression parameters are listed in Table 1. Sample realizations of these fitted profiles are plotted in Figure 6 along with the prescribed profile. The measured and the sampled profiles often differ significantly from the prescribed profile, particularly near the edge of contact.

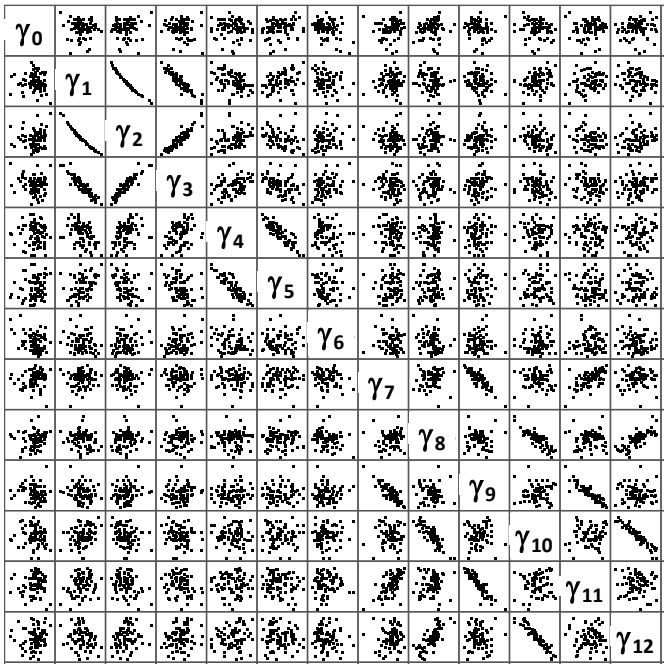

Figure 5. Scatter plots of the profilometry regression parameters, γ_0 through γ_{12}

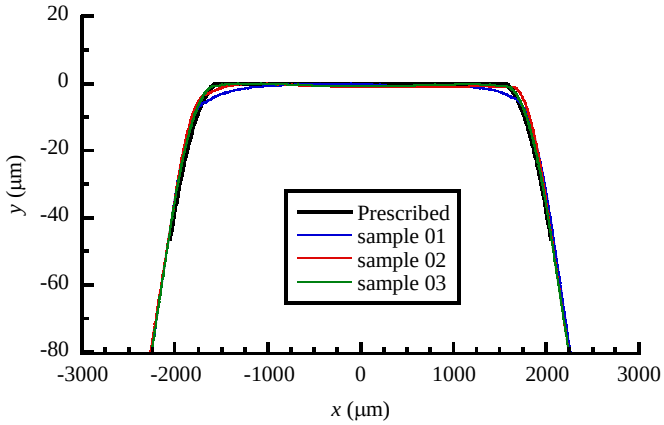

Figure 6. Randomly sampled pad profiles compared to the prescribed profile.

Table 1. Summary of random variable statistics

Random Variable	No.	Mean	St. Dev.	Distribution Type
Initial crack size, a_i (in)	X_1	$5.95\text{x}10^{-4}$	$3.34\text{x}10^{-4}$	Lognormal
Friction coefficient, μ_{ave}	X_2	0.302	0.021	Correlated normal
Partial slip slope, α	X_3	1.96	0.120	ρ_{23} = - 0.375
Crack growth, $\log_{10}(C_1)$	X_4	-12.7	0.486	Correlated normal
Crack growth, n_1	X_5	7.19	0.715	ρ_{45} = -0.9973
Crack growth, $\log_{10}(C_2)$	X_6	-10.1	0.157	Correlated normal
Crack growth, n_2	X_7	3.81	0.146	ρ_{67} = -0.9751
Profile, $\gamma_0 = k^L$	X_8	0.181	$5.84\text{x}10^{-3}$	Correlated normal
Profile, $\gamma_1 = y_0^L$	X_9	-2335	410	
Profile, $\gamma_2 = R^L$	X_{10}	2333	411	
Profile, $\gamma_3 = x_0^L$	X_{11}	-1612	37.7	
Profile, $\gamma_4 = R^R$	X_{12}	2289	379	
Profile, $\gamma_5 = x_0^R$	X_{13}	1620	35.4	
Profile, $\gamma_6 = k^R$	X_{14}	-0.183	$4.96\text{x}10^{-3}$	
Profile, $\gamma_7 = c_1$	X_{15}	$-2.00\text{x}10^{-4}$	$6.20\text{x}10^{-4}$	
Profile, $\gamma_8 = c_2$	X_{16}	$-1.21\text{x}10^{-6}$	$1.01\text{x}10^{-6}$	
Profile, $\gamma_9 = c_3$	X_{17}	$1.53\text{x}10^{-10}$	$6.38\text{x}10^{-10}$	
Profile, $\gamma_{10} = c_4$	X_{18}	$9.80\text{x}10^{-13}$	$6.16\text{x}10^{-13}$	
Profile, $\gamma_{11} = c_5$	X_{19}	$-3.77\text{x}10^{-17}$	$1.87\text{x}10^{-16}$	
Profile, $\gamma_{12} = c_6$	X_{20}	$-3.80\text{x}10^{-19}$	$1.59\text{x}10^{-19}$	

IV. Analysis Methods

A. Monte Carlo Sampling

Monte Carlo sampling was carried out to determine the moments (mean and standard deviation) of the cycles-to-failure. This procedure involved repeated generation of realizations of the random variables and execution of the deterministic fretting fatigue algorithm to determine cycles-to-failure. The deterministic fretting fatigue algorithm was simplified as much as possible to minimize the computational time needed for each set of random variable samples. This included calculation of the contact forces using the method demonstrated by Gean and Farris [6], rather than modeling the contact in a FEM analysis. The CAPRI run time was minimized by reducing the number of Fast Fourier Transform terms to the minimum required and optimizing the solver parameters for this problem. Finally, a linear fit of the bulk stresses as a function of the contact forces was created from a series of FEM analyses, rather than using a new FEM analysis for each Monte Carlo run. Eliminating the FEM analyses from the calculation of fretting fatigue life reduced the computational time to approximately 1.2 s per sample when running in parallel with 4 processors on an Intel Xeon quad core workstation. This made running the Monte Carlo analysis with a significant number of samples possible. The ensemble of cycles to failure, N_f, results were then analyzed to determine the mean and standard deviation. Sufficient samples were executed to ensure high confidence in the computed moments.

B. Sensitivity analysis

Probabilistic sensitivities play an important role in determining insight into the dominant factors governing a probabilistic analysis and provide information as to potentially effective methods to improve the reliability. There are a number of methods in the literature such as scatter plots [12], Pearson or Spearman correlation [13], regression methods [14], and the Score function method [15], among others, that can provide useful information.

1. *Scatter plots*

Scatter plots are a two-dimensional point plot of the sample points version the correspond response points. The sample realizations for each random variable (X) and the corresponding results (Y) are plotted on separate axes. If a random variable is not important, no pattern should be discernable, that is, the samples for X should mimic its

marginal distribution. Conversely, if a random variable is important, the pattern of realizations for X will be distinctly non-random. Scatterplots are an inexpensive but qualitative method.

2. *Regression and correlation*

Linear regression (LR) methods are well known and widely available tools for assessing variance contribution. LR approximates the relationship between response and the random variables as

$$y(\mathbf{x}) = \beta_0 + \sum \beta_i f(x_i) \tag{6}$$

where *f* is an arbitrary function of the random variable *Xi*. In general, LR may contain quadratic and interaction terms of any number of variables. The correlation coefficient (Pearson or Spearman) for each random variable provides an indication of the contribution of that variable's variance to the response variance.

3. *Segmented input distributions*

Sensitivities based upon segmented input distributions involve dividing the input samples into two or more separate groups based on the output samples. The output and related input samples are sorted in ascending values based upon the output results. If the variable has no effect, the distributions in each group will be the same as the marginal distribution. If not, then the variable has a significant effect. Various statistical tests such as Cramer-von Mises, Mann-Whitney, etc. can be employed to determine if the distributions are significantly different.

4. *Score function*

The Score function method computes the partial derivative of the response (cycles-to-failure) with respect to the parameters of the input PDFs. The probabilistic sensitivities (partial derivatives of the response moments (mean and standard deviation) with respect to the parameters of the random variable pdf's) can be obtained for negligible cost Probabilistic sensitivities such as $\partial\mu_Z/\partial\mu_i$ represent the sensitivity of the mean of cycles-to-failure with respect to the mean of random variable *Xi*.

IV. Results

A. Probabilistic Life Prediction

The probabilistic fretting fatigue life prediction tool was exercised at several experimental load cases. Results were generated at the 5 applied loading conditions (F_{max} = 18, 20, 22, 24, and 30 kN) used in the dovetail testing program. Lives were generated at each loading condition using 1000 samples of the random pad profiles, coefficient of friction, and contact force partial slip slope. These results are plotted on lognormal probability paper in Figure 7 along with the experimental lives. The experimental lives shown were as follows: 1,371,000, 10,000,000, and 693,000 cycles at 18 kN; 995,000 and 919,900 cycles at 20 kN; 249,900, 346,200, and 497,800 cycles at 22 kN; 164,000 cycles at 24 kN; and 105,000 cycles at 30 kN. These data were quite limited for an evaluation of a probabilistic life prediction, however, they were still useful to ensure the predictions were near the test results. The comparison in Figure 7 shows that at the higher loads the predictions were closer than at the lower loads. Since the predictions were entirely based on fatigue crack growth from a small crack, this could indicate that a significant period of crack formation could be taking place at the longer lives.

The results plotted in Figure 7 were generated with just 1000 samples to minimize processing

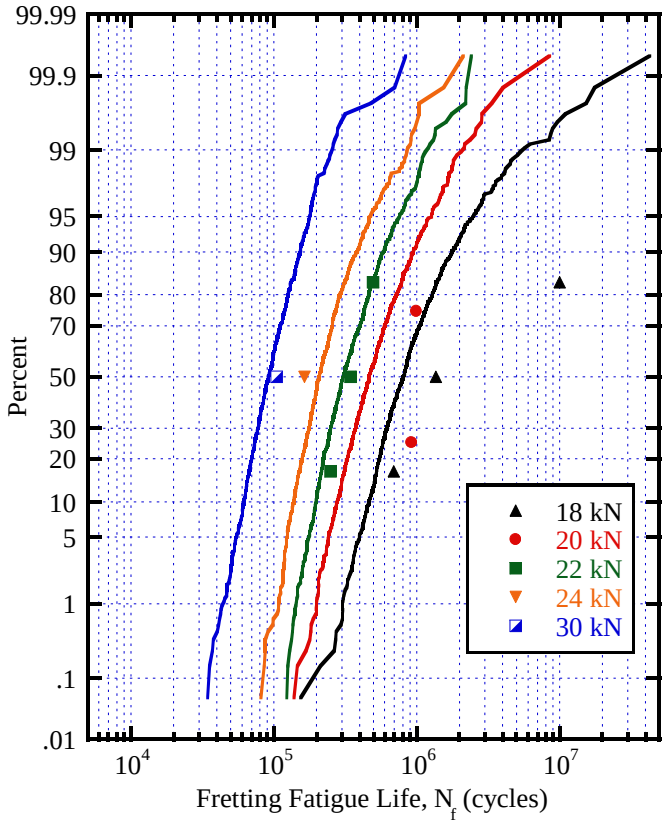

Figure 7. Probability plot of experimental (points) and predicted (lines) lives at several applied loads

time for each condition analyzed. Since the number of samples was relatively small, an understanding of the variance in the estimates of mean and standard deviation of N_f was important. Variance estimates of the modes of the distribution were calculated at each of the applied forces and listed in Table 2. Since the distribution of N_f was fairly lognormal, the modes of the distribution of the logarithm of N_f were calculated. The columns showing the 95% confidence bounds of the mean were then converted back to cycles. The coefficient of variance (COV) was calculated entirely in log units. Interestingly, the COV decreased with increased applied loading, which was consistent with fatigue test results in Ti-6Al-4V [10] and is generally true in metallic aerospace materials. Also, in Table 2 the estimates of the modes of the distribution were calculated for larger numbers of samples at F_{max} = 22 kN. With more samples, the confidence bounds shrink significantly as expected. In addition to quantifying the modes of the distribution, PDF's were fit to the distribution. Figure 8 is a plot of two PDF types fit to the N_f results at F_{max} = 22 kN. The kernel line is a nonparametric estimate of the PDF, while the lognormal curve was fit using the mean and standard deviation of the logarithm of N_f. The differences in the PDF's showed that the distribution of failure lives was weighted toward longer lives. This can also be observed in Figure 7, and this trend increased with lower applied loads.

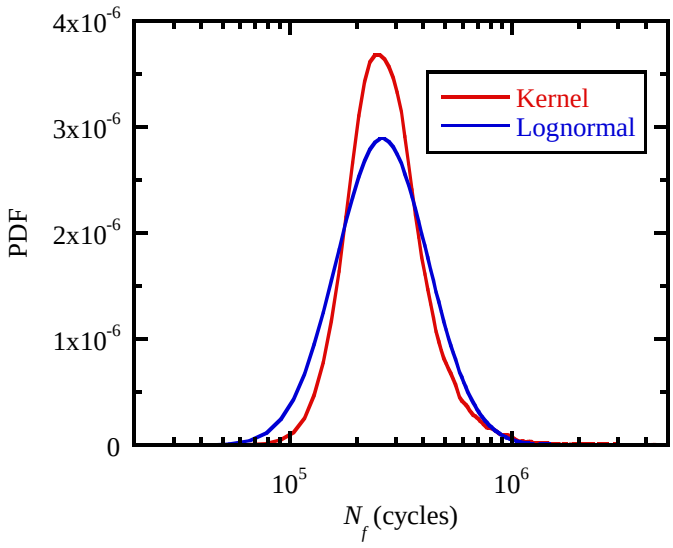

Figure 8. PDF estimates of N_f for 10,000 samples

Table 2. Mean and standard deviation of the Monte Carlo analysis results including confidence bounds

		95% confidence for mean of $\log_{10}(N_f)$ (cycles)			95% confidence for COV of $\log_{10}(N_f)$		
F_{max} (kN)	Samples	Lower	Mean	Upper	Lower	COV	Upper
18 kN	1000	833,200	864,000	895,900	4.11%	4.28%	4.46%
20 kN	1000	480,500	495,600	511,200	3.66%	3.82%	3.98%
22 kN	1000	319,400	328,400	337,700	3.40%	3.54%	3.69%
22 kN	10,000	323,200	326,200	329,200	3.67%	3.72%	3.77%
22 kN	50,000						
24 kN	1000	215,600	221,200	227,000	3.26%	3.40%	3.55%
30 kN	1000	92,900	95,100	97,300	3.08%	3.21%	3.35%

B. Sensitivity Results

1. *Scatter plots and correlations*

Figure 9 below shows the scatter plots that relate cycles-to-failure (y axis) with each random variable (x axis) for 10,000 samples. The scatter plot for random variable X_2 shows a definite pattern. Correlation coefficients (Pearson or Spearman) for each variable relate to the amount of variance in Y that can be apportioned to X_i. The results for Pearson correlation coefficients, given in Table 3, indicate that variable X_2 (coefficient of friction) is by far the dominant variable, contributing 65% of the variance in N_f. It must be pointed out, however, that the correlation coefficients are obtained without consideration for the simultaneous variations in other random variables. A better estimate of variable importance can be determined using linear regression, discussed below.

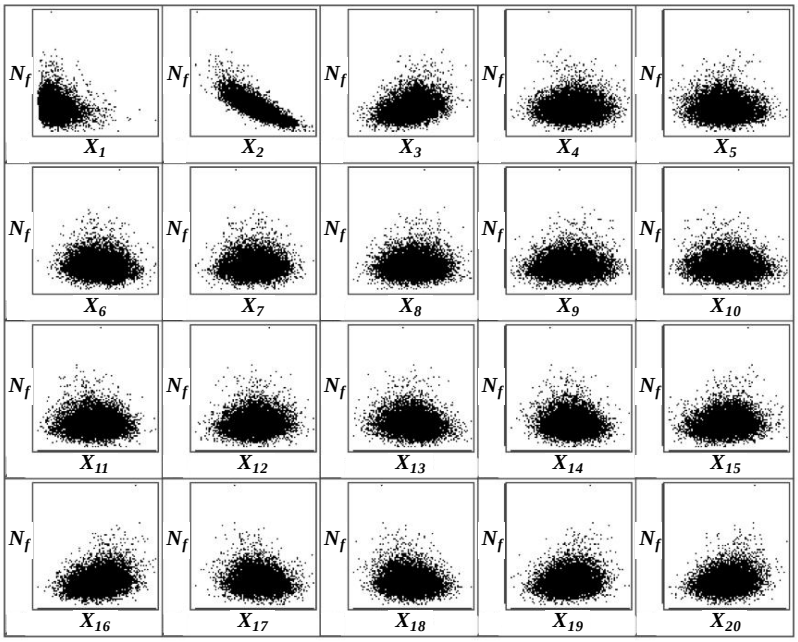

Figure 9. Scatter plots of the model output cycles to failure, N_f, versus the input random variables, X_1 through X_{20}

Table 3. R-squared values for the random variables

Variable	R^2
X_1	0.024
X_2	0.645
X_3	0.093
X_4	0.001
X_5	0.002
X_6	0.006
X_7	0.002
X_8	0.002
X_9	0.004
X_{10}	0.004
X_{11}	0.003
X_{12}	0.005
X_{13}	0.017
X_{14}	0.008
X_{15}	0.007
X_{16}	0.063
X_{17}	0.013
X_{18}	0.020
X_{19}	0.020
X_{20}	0.038

2. *Linear Regression*

In this research, an LR model of the form

$$y(\mathbf{X}) = \beta_0 + \sum \beta_i X_i \tag{8}$$

was used, where $\boldsymbol{X}$ denotes a vector of random variables, y represents the cycles-to-failure and the β's are coefficients that are fit to the analytical results. Table 4 shows the results of a "best model" fit using a specified number of variables. For example, using only 2 variables, the combination of X_2 and X_{16} account for the largest percentage of the variance in N_f. Note, once X_2 is included in the model, adding X_{16} adds 17 percent to the R^2 sum, however, the R^2 value using the Pearson correlation coefficient for X_2 without considering any other random variables is 25%. From the results one can see quickly the diminished returns offered after the first few random variables. For example, if only 5 random variables are used in an LR model, this model would account for 85% out of a possible 91% of the output variance. It is somewhat surprising that a simple linear model with respect to the random variables can account for such a large percentage.

Table 4. Best model linear regression results

Number	R^2	C(p)	Random Variables in Model									
1	0.645	28,370	X_2									
2	0.713	21,020	X_2	X_{16}								
3	0.754	16,620	X_2	X_9	X_{10}							
4	0.824	9000	X_2	X_{16}	X_{18}	X_{20}						
5	0.846	6660	X_1	X_2	X_{16}	X_{18}	X_{20}					
6	0.855	5710	X_1	X_2	X_{13}	X_{16}	X_{18}	X_{20}				
7	0.874	3640	X_1	X_2	X_6	X_7	X_{16}	X_{18}	X_{20}			
8	0.883	2690	X_1	X_2	X_6	X_7	X_{13}	X_{16}	X_{18}	X_{20}		
9	0.898	1060	X_1	X_2	X_6	X_7	X_{16}	X_{17}	X_{18}	X_{19}	X_{20}	
10	0.901	720	X_1	X_2	X_6	X_7	X_{13}	X_{16}	X_{17}	X_{18}	X_{19}	X_{20}

Table 5 shows the results using LR considering natural groupings of random variables. The variables were partioned into 4 groups: (X_1 - initial crack size, X_2-X_3 coefficient of friction – partial slip slope, X_4-X_7 crack growth parameters, X_8-X_{20} geometry profile). The results indicate that group 2 (the coefficient of friction– partial slip slope is dominant followed by the geometry profile. Surprisingly, the traditionally dominant random variables in fatigue, crack growth rate and initial crack size are not significant in terms of their contribution to the output variance, e. g., these parameters could be modeled deterministically.

Table 5. Linear regression group analysis showing the effect of each random variable group on the model R^2

Group	RV Added	# RV	Model R^2	R^2	$C(p)$	F value
1	X_2, X_3	2	0.645	0.645	28,370	9080
2	$X_8 - X_{20}$	15	0.210	0.855	5710	1110
3	$X_4 - X_7$	19	0.030	0.885	2420	660
4	X_1	20	0.022	0.908	20	2410

3. *Segmented Distributions*

10,000 samples were sorted by cycles-to-failure then segmented into three groups: early failures, middle failures, and late failures. That is, samples in the first group failed early (low cycles-to-failure), and samples in the third group failed last, etc. Nonparametric density estimation methods [16] were used to develop PDF's for each random variable for each group of samples and for the total ensemble of samples. Figure 10 shows the PDF's for three random variables that exhibit a large, moderate and minimal effect due to segmentation. The violet, red, and green distributions derive from the early, middle and late cycles-to-failure. The black dashed line indicates the PDF using the total ensemble of samples.)

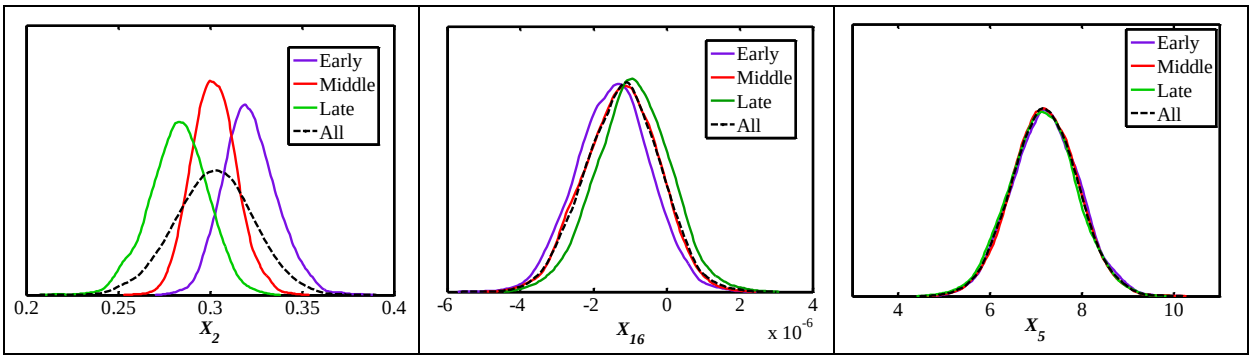

Figure 10. Segmented PDF's showing large (X_2), moderate (X_{16}) and minimal (X_5) effects

V. Summary and Conclusions

A new probabilistic fretting analysis was developed to investigate the relative importance of typical fretting input variables on the predicted failure lives. Several random variable inputs were identified and pdf's were quantified using laboratory data. Monte Carlo sampling of the input pdf's was performed and a deterministic analysis was repeatedly run using the sampled inputs to obtain a distribution of predicted fretting lives. The results showed that significant scatter in fretting lives can be expected based on variability in the material properties, contact profiles, coefficient of friction, and contact force response. Interestingly, the dominant variables in terms of contribution to the cycles-to-failure variance were the coefficient of friction and several terms within the geometry profile; whereas, the traditionally dominant variables, initial crack size and crack growth, were not significant.

Acknowledgements

The authors would like to thank Prof. Farris and his students at Purdue University for providing the CAPRI software used in this study. This work was partially supported by the Air Force Research Laboratory, Materials and

Manufacturing Directorate through subcontract USAF-5212-STI-SC-0021 from General Dynamics Information Technology to the University of Texas at San Antonio.

References

[1]Kumari S, Farris, TN, "Statistical Analysis of Effect of Contact Surface Profile on Fretting Fatigue Life for Ti-6Al-4V," 47th AIAA/ASME/ASCE/AHS/ASC Structures, Structural Dynamics, and Materials Conference, AIAA 2006-1729, 2006.

[2]Zhang R, Mahadevan S, "Probabilistic Prediction of Fretting Fatigue Crack Nucleation Life of Riveted Lap Joints," 41st AIAA/ASME/ASCE/AHS/ASC Structures, Structural Dynamics, and Materials Conference, AIAA-2000-1645, 2000.

[3]Chevalier L, Cloupet S, Soize C, "Probabilistic Model for Random Uncertainties in Steady State Rolling Contact," Wear 2005, 258, pp 1543-1554.

[4]Golden PJ, Nicholas T, "The Effect of Angle on Dovetail Fretting Experiments in Ti-6Al-4V," Fatigue and Fracture of Engineering Materials and Structures, 28, 2005, pp. 1169-1175.

[5]Golden PJ, Calcaterra. A Fracture Mechanics Life Prediction Methodology Applied to Dovetail Fretting. Tribology International, Vol. 39, 2006, pp.1172-80.

[6]Gean, M.C., Farris, T.N., "Mechanics Modeling of Firtree Dovetail Contacts," 49th AIAA/ASME/ASCE/AHS/ASC Structures, Structural Dynamics, and Materials Conference, AIAA 2008-2176, 2008.

[7]McVeigh PA, Harish G, Farris TN, Szolwinski MP. Modeling interfacial conditions in nominally flat contacts for application to fretting fatigue of turbine engine components. International Journal of Fatigue , Vol. 21, 1999; pp. S157–65.

[8]Golden, P.J., Grandt, A.F., Jr., "Fracture mechanics based fretting fatigue life predictions in Ti–6Al–4V," Engineering Fracture Mechanics, Vol. 71, 2004, pp. 2229-2243.

[9]Gallagher JP, et al. AFRL-ML-TR-2001-4159, Improved High-Cycle Fatigue (HCF) Life Prediction, Wright-Patterson Air Force Base, OH, 2001.

[10]Golden, P.J., John, R., Porter, W.J., III, "Variability in Room Temperature Fatigue Life of Alpha+Beta Processed Ti-6Al-4V," International Journal of Fatigue, 2009, doi:10.1016/j.ijfatigue.2009.01.005.

[11]Walker, K., "The Effect of Stress Ratio During Crack Propagation and Fatigue for 2024-T3 and 7075-T6 Aluminium," Effects of Environment and Complex Load History on Fatigue Life (10th edn), ASTM STP 462, American Society for Testing of Materials, PA, 1970, pp. 1–14.

[12]J.P.C.Kleijnen, and J.C. Helton, "Statistical Analyses of Scatterplots to Identify Important Factors in Large-scale Simulation, Review and comparison of techniques," Reliability Engineering and System Safety, 65,1999, pp.147-185.

[13]D.M. Hamby, "A Review of Techniques for Parameter Sensitivity Analysis of Environmental Models," Environmental Monitoring and Assessment 1994, 32, pp 135-154.

[14]N.R. Draper and H. Smith, Applied Regression Analysis, 3rd Ed., Wiley-Interscience, 1998

[15]Rubinstein R.Y. and Shapiro, A. Discrete Event Systems, Sensitivity Analysis And Stochastic Optimization By The Score Function Method. J. Wiley & Sons, Chichester, England, 1993.

[16]B.W. Silverman, Density Estimation for Statistics and Data Analysis, Chapman & Hall/CRC, Baco Raton, FL, 1998.